Indian Journal of Chemistry
Vol. 65, March 2026, pp. 246-254
DOI: 10.56042/ijc.v65i3.24067

Cr(II), Co(II) and Cu(II) complexes with 2-aminodiphenylamine derived Schiff base ligand: Synthesis, characterization, DFT and biological insights

Vishnu Kumar Modanawal[a], Ved Prakash Arya[b], Alok Kumar Maurya[b], Sikandar Paswan[c], Siddharth Agrawal[d], Shekhar Srivastava[a] & Nitesh Jaiswal*[b]

[a] Synthetic Inorganic and Metallo-organic Research Laboratory, Department of Chemistry, University of Allahabad, Allahabad 211 002, Uttar Pradesh, India

[b] Department of Chemistry, Prof. Rajendra Singh (Rajju Bhaiya) Institute of Physical Science for Study and Research, Veer Bahadur Singh Purvanchal University, Jaunpur 222 003, Uttar Pradesh, India

[c] Department of Chemistry, BRD PG College, Deoria 274 001, Uttar Pradesh, India

[d] Synthetic and Natural Products Research Laboratory, Department of Chemistry, CMP Degree College, University of Allahabad, Prayagraj 211 002, Uttar Pradesh, India

E-mail: njchem1@gmail.com

Received 22 September 2025; accepted (revised) 6 March 2026

Two Schiff bases *viz.* 2-(((2-(phenylamino)phenyl)imino)methyl)phenol (L^1H) and 2-methoxy-6-(((2-(phenylamino)phenyl)imino)methyl)phenol (L^2H) have been synthesized by the reaction of 2-aminodiphenylamine with salicylaldehyde and *o*-vanillin in 1:1 molar ratio. A series of transition metal complexes of Cr(II), Co(II) and Cu(II) have been synthesized using Schiff bases (L^1H) and (L^2H) in a 1:2 molar ratios. The newly synthesized ligands and metal complexes have been characterized by elemental analysis and different spectroscopic techniques including FT-IR, UV–Vis, NMR and mass spectrometry. The DFT method has been incorporated to get the electronic properties of ligands and their transition metal complexes. The spectroscopic analysis and computational method indicate distorted octahedral geometry around metal centers. The *in vitro* antimicrobial activities of synthesized ligands and transition metal complexes have been evaluated against *Escherichia coli* and *Staphylococcus aureus*. The results indicate that metal complexes exhibit higher antibacterial activity as compared to free Schiff bases and lower antibacterial activity as compared to the standard drug Gentamycin.

Keywords: Transition metal complexes; Schiff base; 2-aminodiphenylamine; UV-Vis; DFT; Antibacterial studies

The metal ions and its complexes have significant contribution in function of biological system. The metal ions with rationally design organic ligands become significant for several biological applications. The presence of imine functional group (>C=N–) in organic molecule represent a class of ligand namely Schiff base in honor of its discoverer Hugo Schiff. The condensation reaction of aldehydes and amines results in formation of imine derivative ligands. The potential products of primary amine and carbonyl compound and its metal complexes generated a lot of interest among researcher due to its significant pharmacological, physiological, medicinal activities and exciting chelating properties[1,2].

The transition and inner transition metal complexes of bidentate, tridentate or polydentate Schiff bases are key research area for chemist not because of its versatile coordination chemistry but also its wide range of biological applications like antibacterial, antifungal, antioxidant, anticancer and anti-inflammatory properties[3-10]. The coordination chemistry of chromium, cobalt and copper is of considerable interest since their complexes with Schiff bases are reported to be biologically active[11-16]. The salicylaldehyde derivative Schiff base ligands shown significant application in catalysis, materials science, and biological activity[16,17]. Similarly, o-vaniline derivative Schiff base ligands reported for extensive biological activities, which include antibacterial, antiviral and anticancer effects[18-20]. The chelation of salicylaldehyde and *o*-vanilin derivative Schiff base ligands with metal ions further enhance the application potential of metal ions.

The present investigation deals with synthesis and characterization of two tridentate Schiff bases, 2-(((2(phenylamino)phenyl)imino)methyl)phenol (L^1H), 2-methoxy-6-(((2(phenylamino)-imino) methyl) phenol (L^2H). These synthesized ligands were allowed to react

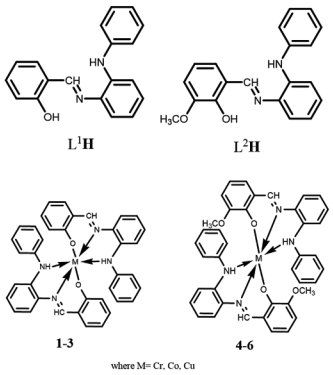

Scheme 1 — Structural representation of ligands and metal complexes

with Cr(II), Co(II) and Cu(II) ions, resulting metal complexes of composition $[M(LnH)_2]$ (where M = Cr(II) (1), Co(II) (2), Cu(II) (3) for n = 1 and M = Cr(II) (4), Co(II) (5), Cu(II) (6) for n = 2) (Scheme 1). Further, these complexes were characterized by spectroscopic techniques such as UV-Vis, FT-IR and ESI-MS. The computation calculations using DFT were carried out for ligands and metal complexes to get insight about the electronic properties. The *in vitro* anti-bacterial properties of synthesized ligands and transition metal complexes were evaluated against *Escherichia coli* and *Staphylococcus aureus.*

Experimental Section

Materials and Methods

Salicylaldehyde, *o*-vanillin, 2-aminodipheny lamine, cobalt(II) chloride, copper(II) acetate, chromium(III) chloride were commercially purchased from Sigma Aldrich and SRL Chemical and all are of reagent grade. The elemental analysis of ligand and metal complexes was performed on Perkin- Elmer 7300 DV CHN-932 elemental analyzer. The UV-Vis spectra of ligands and metal complexes were recorded on a JASCO V-670 UV–Vis spectrophotometer in 200–800 nm range. Bruker FT-IR Spectrometer was used to record IR spectra of ligands and metal complexes using KBr disks over 400-4000 cm^{-1}. The mass spectra of ligands and metal complexes were recorded on Xevo G2-S Q Tof in ESI positive mode. 1H NMR spectra of ligands were recorded on a Bruker Advance –II 400FT spectrometer at 400 MHz.

Computational Method

Gaussian 09 program was employed to investigate quantum mechanical properties of ligands and metal complexes. The quantum mechanical properties such as dipole moment, energy of frontier molecular orbitals and HOMO-LUMO energy gap were calculated using density functional theory (DFT) method. The 6-31G(d, p) basis set at B3LYP level were used to optimized. The ground state geometry of ligand and their metal complexes[21,22].

In vitro Antibacterial Studies

Agar disc-diffusion method[23] was choose to evaluate *in vitro* antibacterial activities of ligands (L^1**H**, L^2**H**) and their metal complexes (**1-6**). The antibacterial activities measured against *gram negative Escherichia coli* and gram positive *Staphylococcus aureus.* The stock solution (1 mg mL^{-1}) of Schiff bases and its metal complexes were prepared in DMSO which is further diluted to 100 μg mL^{-1} with sterilized distilled water. The surface of agar was uniformly incubated with bacteria with 15 hrs. Whatman filter paper (5 mm) was soaked in a test chemical solution made in DMSO and placed on top of the bacterial lawn in order to measure the zone of inhibition. The petri dishes were incubated at 37°C for the entire night in an Equitron, Stream series-091 L incubator. Gentamicin was also screened in the same manner for comparison.

Synthesis of ligands

2-((2-(phenylamino)phenylimino)methyl)phenol (L^1**H)**: A methanolic solution of Salicylaldehyde (1.00 g, 8.18 mmol) dissolved was added to an equi-molar methanolic solution of 2-aminodiphenylamine (1.50 g, 8.18 mmol). The mixture was stirred and refluxed for 4-5 hrs. The product obtained was air dried and recrystallized with hot methanol.

2-methoxy-6-(((2-(phenylamino)phenyl)imino) -methyl)phenol (L^2**H)** : Similar procedure was used for the preparation of 2-methoxy-6-(((2-(phenylamino) phenyl)imino) -methyl)phenol (L^2**H)** by the reaction of *o*-vanillin (1.00 g, 6.57 mmol) and 2-aminodiphenylamine (1.21 g, 6.57 mmol) in methanol solution.

L^1**H**: Yield 70%. m.p.110°C. Anal. Calcd for $C_{19}H_{16}N_2O$: C, 79.14; H, 5.59; N, 9.72. Found: C, 79.20; H, 5.63; N, 9.64%. IR (KBr): (OH) 3406; (NH) 3044; (C=N) 1570; (Ar-O) cm^{-1} 1481; ^{1}H NMR ($CDCl_3$): δ O-H, 10.09; HC=N, 8.69; Ar-H, 7.74-6.49; UV–Vis (λ_{max}, nm): 283(π→π*), 321(n→π*); ESI-MS: *m/z* Calcd 288.35. Found: 287.12.

L^2**H**: Yield 67%. m.p.135°C. Anal. Calcd for $C_{20}H_{18}N_2O_2$: C, 75.45; H, 5.70; N, 8.80. Found: C, 75.50; H, 5.66; N, 8.75%. UV–Vis (λ_{max}, nm): 295(π→π*), 362(n → π*); IR (KBr): (OH) 3416; (C=N) 1598; (Ar-O)1467 cm^{-1}; ^1H NMR ($CDCl_3$): δ O-H, 10.26; HC=N, 8.81; Ar-H, 7.79-6.51; O-CH_3, 3.47; ESI-MS: *m/z* Calcd 318.38. Found: 317.12.

Synthesis of Metal Complexes

All the transition metal complexes (**1–6**) were synthesized according to the following procedure. Synthesis of [Cu(L^1**H**)$_2$]: A methanolic solution of ligand, L^1H (0.45g, 1.56 mmol) was added to methanolic solution of $Cu(CH_3COO)_2.H_2O$ (0.15g, 0.78 mmol) in 2:1 molar ratio. The resulting solution was stirred and refluxed for 6-8 hrs. The product obtained was dried by vacuum rota-vapour and washed several times with methanol.

[Cr(L^1H)$_2$], (1): Yield 71%. m.p.>250°C. Mol. Formula: $C_{38}H_{30}CrN_4O_2$. Anal. Calcd: C, 72.83; H, 4.83; N, 8.94. Found: C, 72.79; H, 4.78; N, 8.22%. UV-Vis (λ_{max}, nm): 280 (π→π*), 359 (n→π*); IR (KBr): (NH) 3399; (C=N) 1591; (Ar-O) 1475; (M-O) 472; (M-N) 461 cm^{-1}; ESI-MS: *m/z* Calcd 626.68. Found: 625.55.

[Co(L^1H)$_2$], (2): Yield 69%. Mol. Formula $C_{38}H_{30}CoN_4O_2$. Anal. Calcd: C, 72.03; H, 4.77; N, 8.84. Found: C, 72.13; H, 4.79; N, 8.72%; UV-Vis (λ_{max}, nm): 286 (π→π*), 354 (n→π*) nm; IR (KBr): (NH) 3429; (C=N) 1592; (C-O) 1467; (M-O) 516; (M-N) 436 cm^{-1}; ESI-MS: *m/z* Calcd 633.62. Found: 634.35.

[Cu(L^1H)$_2$], (3): Yield 60%. Mol. Formula: $C_{38}H_{30}CuN_4O_2$. Anal. Calcd: C, 71.51; H, 4.74; N, 8.78; Cu, 9.96. Found: C, 71.55; H, 4.77; N, 8.72; Cu, 9.90%. UV-Vis (λ_{max}, nm): 306 (π→π*), 360 (n→ π*); IR (KBr): (NH) 3418; (C=N) 1598; (C-O) 1462; (M-O) 515; (M-N) 467 cm^{-1}; ESI-MS: *m/z* Calcd 638.22. Found: 638.85.

[Cr(L^2H)$_2$], (4): Yield 70%. Mol. Formula: $C_{40}H_{34}CrN_4O_4$. Anal. Calcd: C, 69.96; H, 4.99; N, 8.16. Found: C, 69.96; H, 4.99; N, 8.16%. UV-Vis (λ_{max}, nm): 310 (π→ π*), 368 (n→π*); IR (KBr): (NH) 3382; (C=N) 1625; (C-O) 1460; (M-O) 502; (M-N) 464 cm^{-1}; ESI-MS: *m/z* Calcd 686.72. Found: 687.06.

[Co(L^2H)$_2$], (5): Yield 65%. Mol. Formula: $C_{40}H_{34}CoN_4O_4$. Anal. Calcd: C, 69.26; H, 4.94; N, 8.50. Found: C, 69.30; H, 4.96; N, 8.52%. UV-Vis (λ_{max}, nm): 295 (π→π*), 370 (n→π*); IR (KBr): (NH) 3405; (C=N) 1585; (C-O) 1455; (M-O) 487; (M-N) 425 cm^{-1}; ESI-MS: *m/z* Calcd 693.66. Found: 693.05.

[Cu(L^2H)$_2$], (6): Yield 69%. Mol. Formula: $C_{40}H_{34}CuN_4O_4$. Anal. Calcd: C, 68.80; H, 4.91; N, 8.02; Cu, 9.10. Found: C, 68.85; H, 4.96; N, 8.12; Cu, 9.15%. UV-Vis (λ_{max}, nm): 299 (π→π*), 365 (n→π*); IR (KBr): (NH) 3423; (C=N) 1646; (C-O) 1453; (M-O) 512; (M-N) 443 cm^{-1}; ESI-MS: *m/z* Calcd 698.28. Found: 697.82.

Result and Discussion

The present work deals with synthesis and spectroscopic characterization of chromium, cobalt and copper complexes with two NNO donor tridentate Schiff base ligands (L^1**H**, L^2**H**). The ligands prepared by the condensation reaction between salicylaldehyde, *o*-vanillin with 2-aminodiphenylamine. These synthesized ligands were utilized to produce metal complexes having formula [M(L^nH)$_2$] (where M = Cr(II) (**1**), Co(II) (**2**), Cu(II) (**3**) for n = 1 and M = Cr(II) (**4**), Co(II) (**5**), Cu(II) (**6**) for n = 2].

IR Spectra

Infrared spectroscopy helps in identify functional group and coordination mode present in ligands and metal complexes. The IR spectra (Fig. 1) of ligands and metal complexes were compared to find coordination mode of ligands to metal as result of the complexation[24]. The presence of phenolic OH group cause appearance of vibrational band around 3416 and 3406 cm^{-1}, respectively in ligand L^1**H** and L^2**H**. This band disappears in metal complexes suggest deprotonation of -OH group and formation of bond between oxygen to metal ions[25]. This oxygen metal (M←O) coordination in metal complexes were further supported by the appearance of new band in the region 472-516 cm^{-1}. The appearance of phenolic (C-O) group band at lower wavenumber around 1453-1475 cm^{-1} in complexes also supports coordination of oxygen to metal ions[25]. The characteristic band of azomethine group *(*-C=N) of ligands appeared at 1598 and 1570 cm^{-1} for ligand L^1**H** and L^2**H** respectively. This band appeared with wave number shift in metal complexes which indicate coordination of azomethine nitrogen to metal. This nitrogen metal (M←N) bonding in metal complexes was further established by the presences of new bands in the regions 425-467 cm^{-1} (Ref. 27,28). The

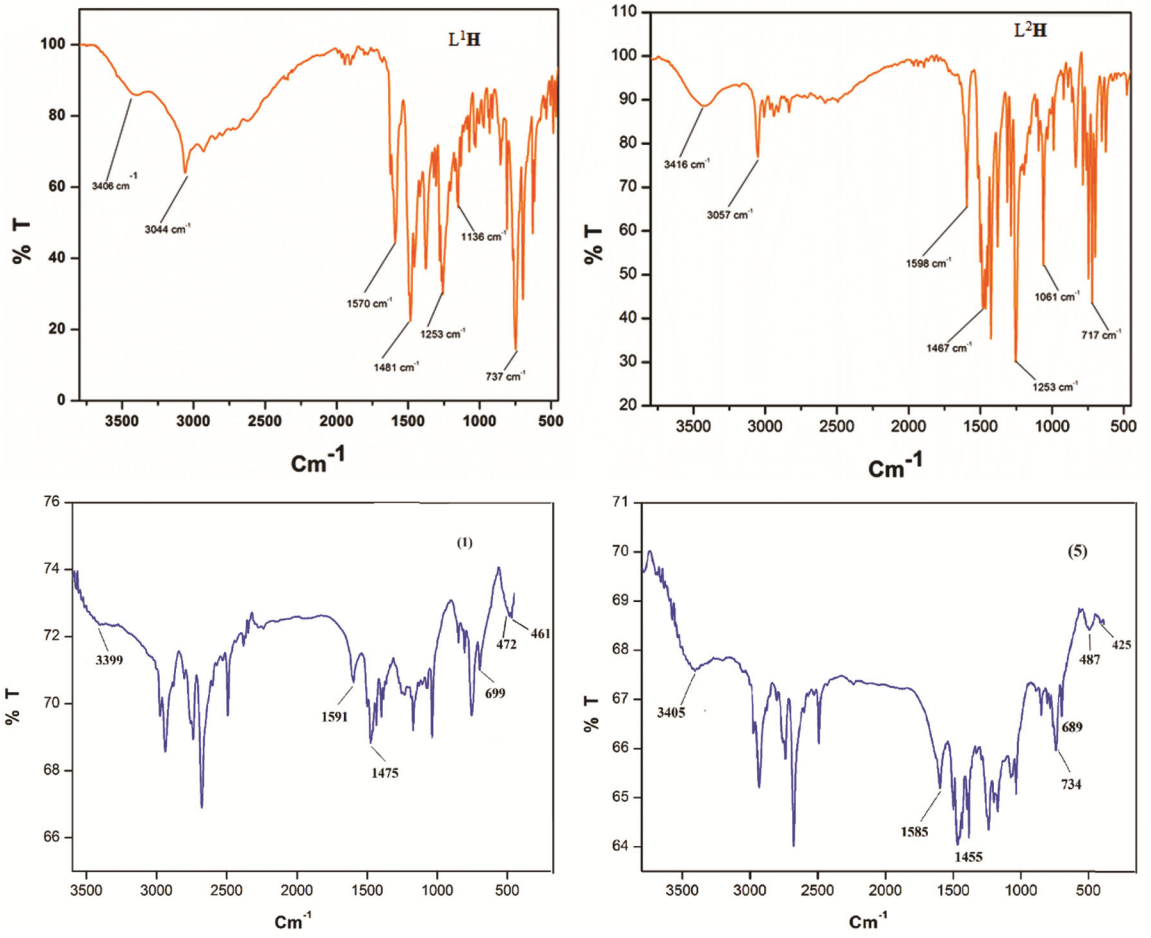

Fig. 1 — IR spectra of L^1**H**, L^2**H** ligands and their Cr(II) (**1**) and Co(II) (**5**) complexes

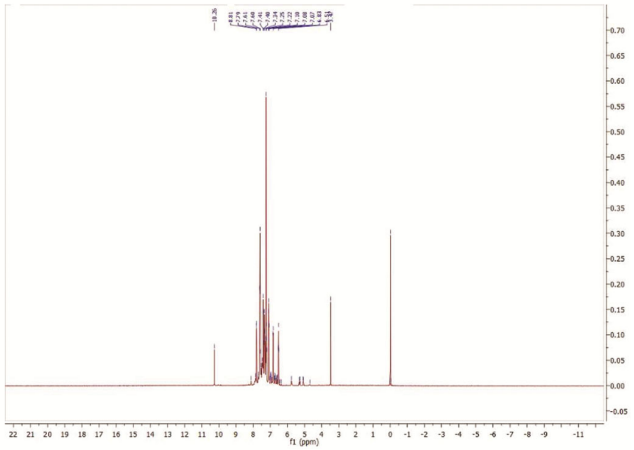

Fig. 2 — ^{1}H NMR spectrum of ligand, L^2**H**

stretching vibration of the (NH) group was found between 3382 and 3429 cm^{-1} (Ref. 29).

NMR spectra

The ^{1}H NMR spectra of ligands were recorded in $CDCl_3$ solution (Fig. 2). The signal appeaed as a singlet at 8.69 ppm and 8.81 ppm in L^1H and L^2H, respectively were ascribed to characteristic azomethine hydrogen CH=N (Ref. 26). Both the ligands showed multiple signals in region 7.74-6.49 ppm and 7.79–6.51 ppm, respectively, due to the aromatic hydrogen atoms. The signal observed at 3.83–3.47 ppm is due to –OCH3 group present in the ligand, L^2H.

UV-Vis spectra

The UV-Vis spectra of ligands and their metal complexes were obtained in DMSO solution in range 200-800 nm at room temperature (Fig. 3). The ligand, L^1**H** shows three absorption bands with maxima at 283, 321 and 359 nm[30]. The absorption band at 283 may correspond to the π→π* transition of azomethine group (-C=N) while the absorption band at 321 nm may correspond to the n→π* transitions associated with azomethine groups which is overlapped with intramolecular charge transfer from aromatic moiety[31]. The ligand (L^2**H**) shows two bands at 295 and 362 nm were attributed to π→π* of

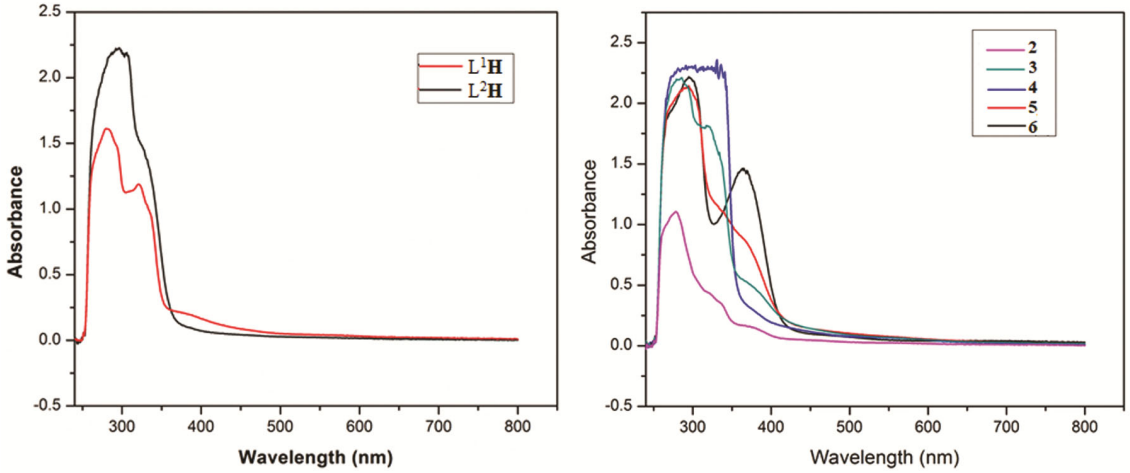

Fig. 3 — UV-Vis spectra of L^1**H**, L^2**H** ligands and their metal complexes (**2-6**)

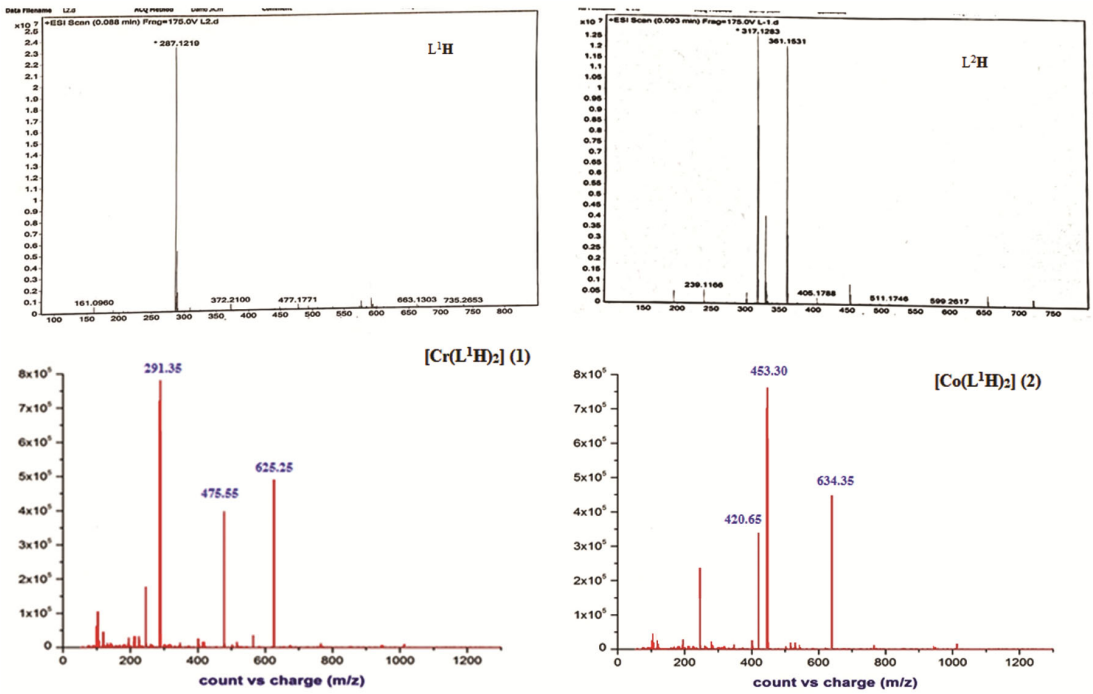

Fig. 4 — Mass spectra of L^1**H**, L^2**H** Schiff bases and their Cr(II) (**1**) and Co(II) (**2**) complexes

benzene ring and n→π* transition state associated with azomethine group with an intra-molecular charge transfer from phenyl ring[32].

The UV-Vis absorption spectra of all the metal complexes show similarities, which show resemblance in the structures of all the complexes. The absorption bands of complex Co(II) **2**, Cu(II) **3**, Cr(III) **4** and Cu(II) **6** are slightly shifted to longer wavelengths (red shift) as compared to free ligand. The absorption bands of complex Cr(III) **1** and Co(II) **5** are shifted to shorter wavelength (blue shift) as compared to free ligand.

The appearance of new absorption bands in range 280-368 nm in metal complexes were attributed to the electron transfer from the transition metal ions to the coordinated ligand it means that charge transfer band from M→L[33]. These modifications in the wavelengths and intensities of ligands and their metal complexes indicate the coordination of ligand to the metal ion.

Mass Spectrometry

The mass spectral data of Schiff bases and their metal complexes were recorded and spectra were shown in Fig. 4. The molecular ion peaks of ligands

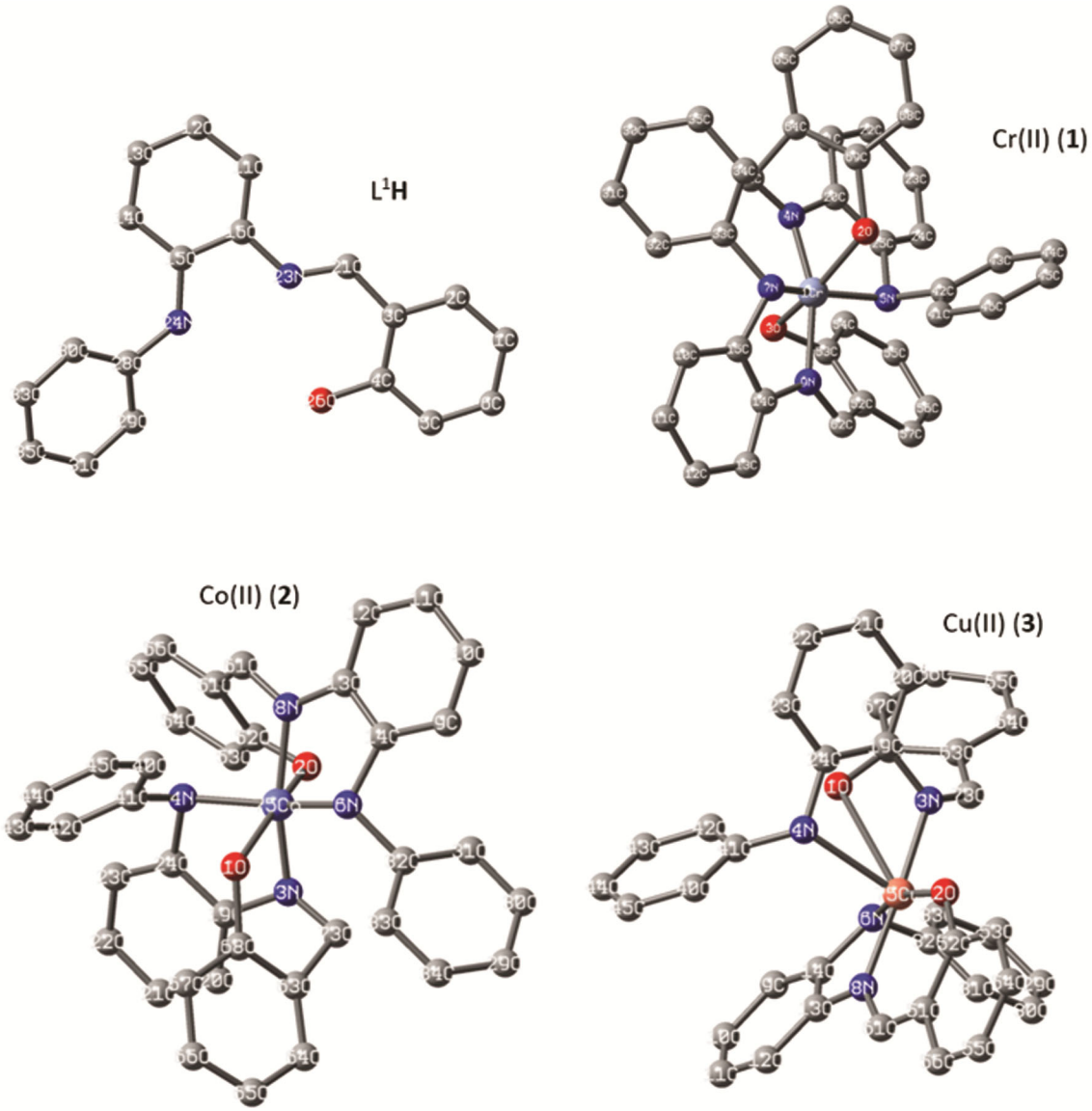

Fig. 5 — The ground state optimized geometry with atom labelling of L^1**H** ligand, Cr(II) (**1**), Co(II) (**2**) and Cu(II) (3) complexes

L^1**H** and L^2**H** were observed at 287.12 and 317.12, respectively. The molecular ion peaks of complexes were observed at *m/z* 625.25 (Calcd 626.68) and 634.35 (Calcd 633.62) for complex $[C_{38}H_{30}CrN_4O_2]$, (**1**) and $[C_{38}H_{30}CoN_4O_2]$ (**2**), respectively.

In these spectra, the base peak observed due to fragment $[C_{14}H_{12}\ CrN_2O_2]^{\cdot+}$ at *m/z* 291.35 (Calcd 292.25) for complex **1** and $[C_{26}H_{20}CoN_2O_2]^{+\cdot}$ at *m/z* 453.30 (Calcd 451.40) for complex **2**. In the complex **1** and **2,** the other important peak were also observed at *m/z* 475.55 (Calcd 474.48) and 420.65 (Calcd 422.06) correspond to the formation of $[C_{26}H_{22}CrN_4O_2]^{\cdot+}$ and $[C_{26}H_{22}CoN_2O_2]^{\cdot+}$, respectively.

Computational Studies

Computational investigations provide a substantial support to the observed experimental result. The computational methods help in analyzing the different electronic properties as well as energy of frontier molecular orbitals. A much effort has been put to grow single crystal but attempts were not successful. Therefore, computation analysis plays very significant role in the structure determination of complexes. The density functional theory (DFT) method was employed at B3LYP level with 6-31G (d, p) basis set to optimized the geometry of ligand and their metal complexes[30,34]. Fig. 5 shows the optimized molecular structure of ligand and their metal complexes with

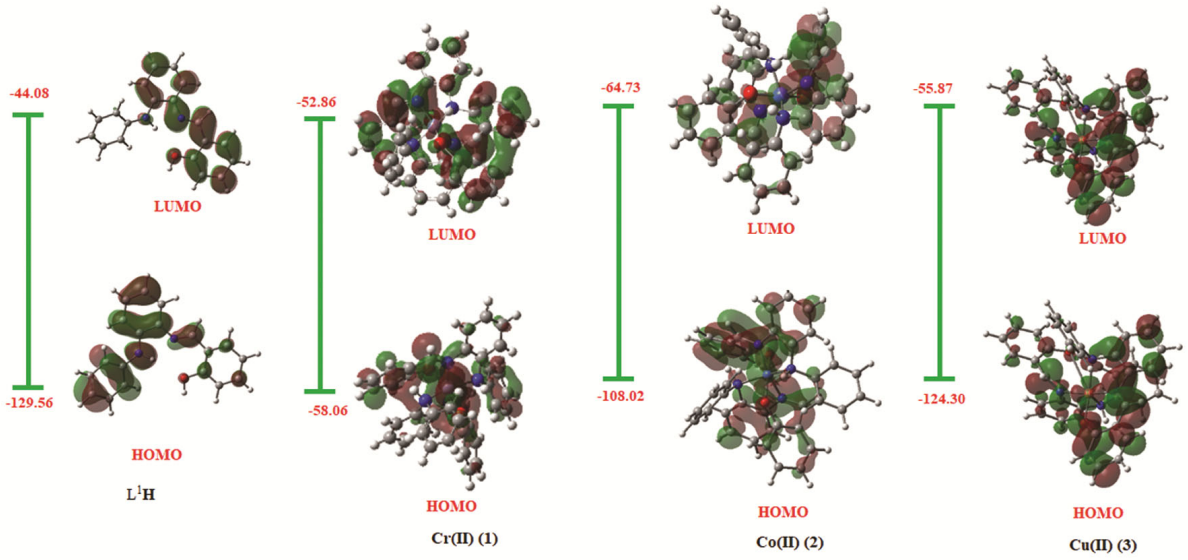

Fig. 6 — Energy diagram of frontier molecular orbitals HOMO and LUMO of ligand (L^1**H**), Cr(II) (**1**), Co(II) (**2**) and Cu(II) (**3**) complexes derived from DFT calculations using B3LYP/6-31G(d, p) level of theory

Table 1 — Computed electronic properties of Schiff base ligand (L^1**H**) and their Cr(II) (**1**), Co(II) (**2**) and Cu(II) (**3**) complexes

S. No.	Compd	Total Energy (eV)	Dipole moment (D)	HOMO (eV)	LUMO (eV)	HOMO-LUMO Energy gap
1	L^1**H**	–24,983.58	3.0841	–129.56	–44.08	–85.48
2	$[Cr(L^1H)_2]$ (**1**)	–78,337.46	3.2914	–58.06	–52.86	–5.20
3	$[Co(L^1H)_2]$ (**2**)	–87,551.59	1.9342	–108.02	–64.73	–43.29
4	$[Cu(L^1H)_2]$ (**3**)	–94,562.85	1.8157	–124.30	–55.87	–68.43

atom labelling. Fig. 6 depicts the highest occupied molecular orbital (HOMO) and the lowest unoccupied molecular orbital (LUMO) of ligand and respective complexes. The values of different electronic properties such as dipole moment, energy band gap are summarized in Table 1 and selected bond lengths and bond angles are summarized in Table 2.

The theoretically calculated values of different bond lengths in metal complexes are compared with the reported metal complexes of similar type. The comparison shows a close agreement in the bond length and bond angle values reported form crystal X-ray data of Cr(II), Co(II) and Cu(II) complexes[35]. The stability of metal complexes with respect to ligand can be predicted on the basis of HOMO and LUMO energy gap. The stability of complexes was further confirmed by the comparison of total energy (E) and energy gap (ΔE) of ligands and complexes.

In vitro antibacterial studies

The disc diffusion method was used to measure *in vitro* anti-bacterial activity of the ligands and its complexes in DMSO solvent against *E. coli* and *S. aureus*[22]. The results of antibacterial activity measurements are presented in Table 3. Both the ligands L^1H and L^2H show moderate activities with zone of inhibition of range 8-14.4 mm. The complexes Co(II) (2), Cu(II) (6) and Cu(II) (3) are found to be inactive against *S.aureus* and *E.Coli,* respectively. The excellent activity shown by Cr(II) (1) and Co(II) (5) complexes with zone of inhibition 16.4 mm and 15.5 mm, against *S.aureus* and *E.coli*, respectively. The Cr(II) (4) complex exhibits moderate activity against both the bacteria. The variation in the antibacterial activities values of Schiff bases and their metal complexes indicated the complexation of ligands to metal ions. From the table, it may conclude that the metals complexes exhibit higher activity as compared to free Schiff base ligands. The effect of metal(II) ions on the cell membrane of bacteria may responsible for the higher activity of metal complexes as compared to free ligands[36]. The higher antibacterial activities also explained by chelation effect as metal chelates formed on the coordination of Schiff bases with metal ions[37].

Table 2 — Selected structural parameters for ligand (L^1**H**) and their Cr(II) (**1**), Co(II) (**2**) and Cu(II) (**3**) complexes at DFT/B3LYP level of theory

Complex	Bond length (Å)		Bond angle (°)	
L^1**H**	21C=23N	1.2887	23N-21C-22H	122.2553
	15C-24N	1.3850	15C-24N-25H	111.5334
	4C-26O	0.9782	4C-26O-27H	110.2934
	16C-23N	1.4008	–	–
	21C-3C	1.4614	–	–
$[Cr(L^1H)_2]$ (**1**)	1Cr-2O	1.8644	7N-1Cr-5N	149.8500
	1Cr-3O	1.7665	9N-1Cr-4N	161.1145
	1Cr-9N	1.8765	3O-1Cr-2O	155.0590
	1Cr-7N	1.8886	4N-1Cr-2O	70.9697
	1Cr-4N	1.7107	4N-1Cr-3O	91.0426
	1Cr-5N	1.8180	3O-1Cr-9N	75.3365
$[Co(L^1H)_2]$ **(2)**	75Co-3N	1.7400	6N-75Co-4N	147.0763
	75Co-4N	1.8952	8N-75Co-3N	165.6150
	75Co-6N	1.9895	3N-75Co-4N	96.1175
	75Co-1O	1.9831	4N-75Co-8N	93.3405
	75Co-2O	1.9315	8N-75Co-6N	81.2062
	75Co-8N	1.8784	6N-75Co-3N	96.4377
$[Cu(L^1H)_2]$ **(3)**	75Cu-2O	1.9312	6N-75Cu-1O	47.4990
	75Cu-8N	1.9773	1O-75Cu-3N	50.3571
	75Cu-6N	2.0943	3N-75Cu-4N	80.9176
	75Cu-4N	2.3644	4N-75Cu-2O	94.3306
	75Cu-3N	2.0046	2O-75Cu-8N	91.2706
	75Cu-1O	3.7612	1O-75Cu-2O	144.8524

Table 3 — The diameters of zone of inhibition of Schiff bases (L^1**H**, L^2**H**) and their metal complexes.

S. No.	Complex	Inhibition zone diameter (mm)	
		E. coli	*S. aureus*
1	(L^1**H**)	8	9
2	(L^2**H**)	11	14.4
3	$[Cr(L^1H)_2]$ (**1**)	12	16.4
4	$[Co(L^1H)_2]$ (**2**)	13	N
5	$[Cu(L^1H)_2]$ (**3**)	N	11
6	$[Cr(L^2H)_2]$ (**4**)	12	13
7	$[Co(L^2H)_2]$ (**5**)	15.5	12.1
8	$[Cu(L^2H)_2]$ (**6**)	13	N
9	Gentamycin [a]	17.5	18.9

[a] Standard drug

This metal chelates suitable for permeation into cells and tissues. The chelation phenomena help in increasing delocalization of π-electrons over the entire chelate ring which ultimately enhances the penetration potency of the complexes into lipid membranes[38,39]. It also increases the hydrophilic and lipophilic nature of the central metal ions, probably leading to liposolubility and permeability through the lipid layer of cell membranes.

Conclusion

We have reported six newly synthesized Cr(II), Co(II) and Cu(II) complexes (**1-6**) with 2-(((2-(phenylamino)phenyl)imino)methyl)phenol (L^1**H**) and 2-methoxy-6-(((2-(phenylamino)phenyl)imino) methyl) phenol (L^2**H**). The synthesized ligands and metal complexes were characterized by elemental analysis and different spectroscopic techniques including vibrational spectroscopy, electronic spectroscopy,

nuclear magnetic resonance spectroscopy and mass spectrometry. DFT calculations of ligands and complexes were performed to explore quantum mechanical properties using B3LYP method and 6-31G (d, p)/LanL2DZ basis set. The experimental and computational results indicate tridentate NNO donor capacity of Schiff base ligands. On the basis of experimental and computational observation a distorted octahedral geometry was proposed for metal complexes. The antibacterial screening of complexes shows low to moderate activity against *Escherichia coli* and *Staphylococcus aureus*.

Acknowledgement

The author, Nitesh Jaiswal would like to express gratitude to University Grant Commission, New Delhi for financial support under startup research grant (No.F.30-573/2021(BSR). Authors acknowledge the Head, Department of Chemistry, University of Allahabad and Head, Department of Chemistry, Prof. Rajendra Singh (Rajju Bhaiya) Institute of Physical Science for Study and Research, Veer Bahadur Singh Purvanchal University, Jaunpur for experimental and Characterization facilities. The authors are thankful to the Material Research Centre, MNIT Jaipur for their kind support in spectroscopic analysis.

Competing interests

The authors declare there are no competing interests.

Data Availability Statement

The authors declare that the data supporting the findings of this study are available within the paper.

References

1 Kanwal A, Parveen B, Ashraf R, Haider N, Ali K G & Attia B, *J Coord Chem*, 75 (2022) 2533.
2 Boulechfar C, Ferkous H, Delimi A, Djedouani A, Kahlouche A, Boublia A, Darwish A A S, Lemaoui T, Verma R & Benguerba Y, *Inorg Chem Comm*, 150 (2023) 110451.
3 Modanawal V K, Paswan S, Anjum A, Kumar M, Srivastava S & Jaiswal N, *J Coord Chem*, 74 (2021) 3140.
4 Paswan S, Anjum A, Yadav N, Jaiswal N & Singh R K P, *J Coord Chem*, 73 (2020) 686.
5 Kumar S, Dhar D N & Saxena P N, *J Sci Ind Res*, 68 (2009) 181.
6 Joseyphus R S & Nair M S, *Mycobiology*, 36 (2008) 93.
7 Savini L, Chiasserini L, Gaeta A & Pellerano C, *Bioorg Med Chem*, 10 (2002) 2193.
8 Karakas A, Elmali H, Unver H & Svoboda I, *J Mol Struc*, 702 (2004) 103.
9 Holla B S, Veerendra B, Shivananda M K & Poojary B, *Eur J Med Chem*, 38 (2003) 759.
10 Gupta K C & Sutar A K, *Coord Chem Rev*, 252 (2008) 1420.
11 Khan M I, Khan A, Hussain I, Khan M A, Gul S, Iqbal M, Ur-Rahman I & Khuda F, *Inorg Chem Comm*, 35 (2013) 104.
12 Ahmed I S & Kassem M A, *Spectrochim Acta A*, 77 (2010) 359.
13 Garnovskii A D, Nivorozhkin A L & Minkin V I, *Coord Chem Rev*, 126 (2003) 1.
14 Badwaik V B, Deshmukh R D & Aswar A S, *J Coord Chem*, 62 (2009) 2037.
15 Yan Z H, Li D & Yin X B, *Sci Bull*, 62 (2017) 1344.
16 Kumar M, Singh A K, Singh A K, Yadav R K, Singh S, Singh A P & Chauhan A, *Coord Chem Rev*, 488 (2023) 215176.
17 Kumar M, Singh A K, Yadav V K, Singh R K, Singh A P & Singh S, *Coord Chem Rev*, 505 (2024) 215663.
18 Andruh M, *Dalton Trans*, 44 (2015) 16633.
19 Gurusamy S, Sankarganesh M, Revathi N, Asha R N & Mathavan A, *J Mol Liq*, 369 (2023) 120941.
20 Singh K, Barwa M S & Tyagi P, *Eur J Med Chem*, 41 (2006) 147.
21 Burgner A, Dolg M, Kuechle W, Stoll H & Preuss H, *Mol Phys*, 80 (1993) 1431.
22 Becke A D, *J Chem Phys*, 104 (1996) 1040.
23 Yadav N, Jaiswal A K, Dey K K, Yadav V B, Nath G, Srivastava A K & Yadav R R, *Mat Chem Phys*, 218 (2018) 10.
24 Pramanik H A R, Paul P C, Mondal P & Bhattacharjee C R, *J Mol Struc*, 1100 (2015) 496.
25 Mahmoud W H, Mohamed G G & El-Dessouky M M, *J Mol Struc*, 1082 (2015) 12.
26 El-Ghamry M A, Elzawawi F M, Aziz A A A, Nassir K M & Abu-El-Wafa S M, *Sci Rep*, 12 (2022) 17942.
27 Raman N, Ravichandran S & Thangaraja C, *J Chem Sci*, 116 (2004) 215.
28 Temel H & Sekerci M, *Synth React Inorg Met Org Chem*, 31 (2001) 849.
29 Muglu H, *Res Chem Intermed*, 46 (2020) 2083.
30 Abou-Hussen A A A & Linert W, *Synth React Inorg Met Org Chem*, 39 (2009) 570.
31 Zhang Z H, Song Y, Okamura T A, Hasegawa Y, Sun W Y & Ueyama N, *Inorg Chem*, 45 (2006) 2896.
32 Fleck M, Karmakar D, Ghosh M, Ghosh A, Saha R & Bandyopadhyay D, *Polyhedron*, 34 (2012) 157.
33 Kumar V, Ntwaeaborwa O M, Soga T, Dutta V & Swart H C, *ACS Photonics*, 4 (2017) 2613.
34 Guo L, Wu S, Zeng F & Zhao J, *Eur Poly J*, 42 (2006) 1670.
35 Reiss A, Cioater N, Dobritescu A, Rotaru M, Carabet A C, Parisi F, Ganescu A, Dabuleanu I, Spinu C I & Rotaru P, *Molecules*, 26 (2001) 3062.
36 Ejidike I P & Ajibade P A, *Molecules*, 20 (2015) 9788.
37 Joseyphus R S & Nair M S, *Mycobiology*, 36 (2008) 93.
38 Neelakantan M A, Marriappan S S, Dharmaraja J, Jeyakumar I & Muthukumaran K, *Spectrochim Acta A*, 71 (2008) 628.
39 Thangadurai T D & Natarajan K, *Trans Met Chem*, 26 (2001) 500.